Journal of the European Ceramic Society 19 (1999) 2155–2163

PII: S0955-2219(99)00029-1
0955-2219/99/$ - see front matter

Development of SiC–Si Composites with Fine-grained SiC Microstructures

Matthias Wilhelm,* Martin Kornfeld and Werner Wruss

Institute for Chemical Technology of Inorganic Materials, University of Technology of Vienna, Austria

(Received 10 November 1998; accepted 12 January 1999)

Abstract

This work summarises the influence of the original particle-size of the SiC powder on the mechanical properties of silicon infiltrated SiC (SiC-Si) composite. These composites are based on a defined SiC particle-size structure. Using α-SiC powders with a mean particle-size of 12·8, 6·4, 4·5 and 3 μm, a clear linear enhancement of the bending strength with decrease of SiC-particle-size was observed. However, a further decrease of the SiC particle-size (from 3 to 0·5 μm) brought no increase of the strength and toughness, respectively. © *1999 Elsevier Science Limited. All rights reserved*

Keywords: silicon infiltration, composites, microstructure-final, mechanical properties, SiC.

1 Introduction

Due to their outstanding mechanical and chemical properties the industrial significance of ceramic materials has increased steadily during the last 10 years. A particularly well known industrial ceramic is silicon-infiltrated silicon-carbide (SiSiC, SiC–Si). This ceramic is produced by infiltrating a porous SiC-C green-product with liquid silicon. The material obtained provides outstanding properties. The high hardness of the SiC in combination with the good resistance against oxidation and corrosion of both silicon and SiC result in excellent wear-resistance. Due to its good tribological properties, high strength at high temperature, low thermal expansion coefficient and excellent thermal shock resistance this ceramic is used in a number of different industrial applications e.g. as a material for combustion chambers, gas-turbines, heat-exchangers, pump-sealing, welding-nozzles, etc.[1–6]

Compared to other ceramic materials the production costs and the costs of the raw-materials to produce SiC-Si are low. The easy machining, the near-net-shape fabrication at low temperatures and the fact that this ceramic shows no shrinkage during production makes this ceramic very attractive. However, the main limiting factor in using this ceramic is its brittleness.

In recent years many efforts have been undertaken to improve the mechanical properties of SiC–Si. Usually SiC–Si ceramics are fabricated by infiltrating a porous compact of α-silicon carbide (SiC) and carbon with liquid silicon (Si). It is well known[7] that one limiting factor to get such ceramics of high strength is the amount of free silicon in the composites. To obtain better mechanical properties and to reduce the amount of free silicon, SiC–Si composites made of two SiC powders with different grain sizes (13 and 3 μm, bimodal SiC structure) were produced.[10] These composites showed low free silicon content but their bending strength was limited at 350 MPa.

In earlier investigations[8] composites made of one SiC powder (monomodal SiC structure) showed that it would be possible to enhance mechanical properties of SiC–Si by reducing the grain size of the SiC used. Schmid (1988)[9] used submicron SiC-powder which caused incomplete compaction and, as a result, porous ceramics were obtained so that no measurements of the strength could be carried out.

In this work we have studied the dependence of the mechanical properties of the final ceramics on the grain size of the original SiC powder. The effects of submicron SiC powders on the bending strength were analyzed.

2 Experimental Procedure

Eight α-SiC powders with a particle-size in the range of 12·8 to 0·24 μm were used to produce the composites. The SiC powders were provided by two suppliers, ESK Kempten Germany (Producer

*To whom correspondence should be addressed. Fax: +43-1-587-7918; e-mail: mwilhelm@fbch.tuwien.ac.at

Table 1. Characteristics of the SiC-Powders used

	SiC-quality	*Mean-SiC-particle-size* [μm]	*Mean SiC particle size after infiltration* [μm]	*Oxygen content [wt%]*
Producer I (ESK)	F 500	12·8	12·1	—
	F 800	6·5	—	—
	F 1000	4·5	—	—
	F 1200	3·0	2·7	0·2
Producer II (H.C. Starck)	UF-05	1·5	1.3	0·8
	UF-10	0·9	—	0·7
	UF-15	0·51	0·8	1·7
	UF-45	0·24	—	4·5

I) and H.C. Starck, Waldshut-Tiengen, Germany (Producer II). The term Fine-SiC as used in this work is defined for α-SiC powders provided by Producer I, the term UF-SiC is used to define α-SiC powder provided by Producer II. The SiC powders provided by Producer I (Fig. 1) consisted of well crystallised particles and were not agglomerated. However, the SiC powders provided by Producer II (Fig. 2) consisted of spherical particles with a relatively wide particle-size distribution and showed agglomeration. Table 1 shows the typical characteristics of the SiC powders used.

The particle-size of the SiC powders used was carried out semi-automatically with the computer program Kontron KS100 by Zeiss: Based on SEM images the SiC particles (about 130 for each SiC powder) were surrounded with a digitiser pen to get digitised values for the particle-perimeter. From these values the mean particle-sizes of the SiC powders were then calculated.

The typical composition of the green compact consisted of 85 wt% α-SiC, 10 wt% phenolformaldehyde resin and 5 wt% soot. Phenolformaldehyde resin was used as an organic binder for the SiC-C compact. The effects of binder material regarding to carbon residue after thermal cracking and binder mobility were investigated in previous works.[10]

To destroy agglomerates in SiC-powder with a particle-size of 0.51 and 0.24 μm, respectively, attrition milling was used. To produce a green-compact the SiC-powder and the soot were suspended in acetone and were homogenised for 24 h in a tumbling mixer. The organic binder was then added and the acetone was removed to obtain a dry product. The dried powder-mixture was sieved, granulated by rolling the moist powder in a flask and then dry pressed at 75 MPa to get green-compact measuring approximately $50\times40\times4\,mm^3$.

After pressing, the green-compact was heated up under controlled conditions. During heating the organic binder hardened and cracked to pure carbon. After hardening and cracking in different furnaces the weight and the dimensions of the green-compacts were measured. The subsequent infiltration procedure (contact-infiltration technique) was carried out in a graphite furnace under vacuum (typically 5×10^{-5} bar) at 1600 °C. In this technique, an infiltrant composed of silicon and organic binder is placed on top of the green-compact.

During heating the silicon melts and flows into the green-compact. There it reacts with the soot and the carbon residue, generated by the cracked organic binder, forming secondary β-SiC.[11] This formation is exothermic. The newly formed β-SiC

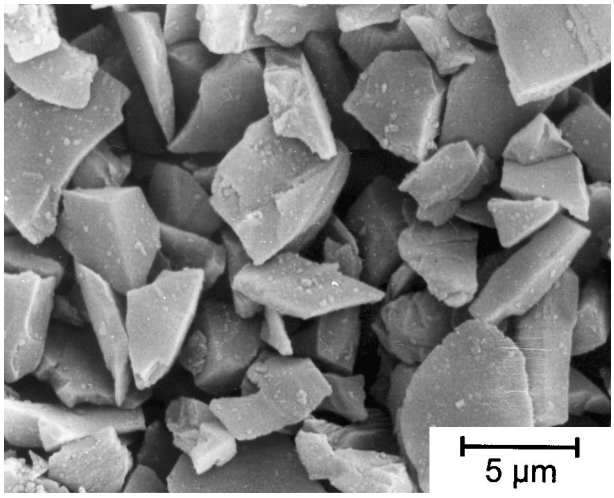

Fig. 1. SEM-image of fine-SiC powder with a mean particle-size of 3 μm.

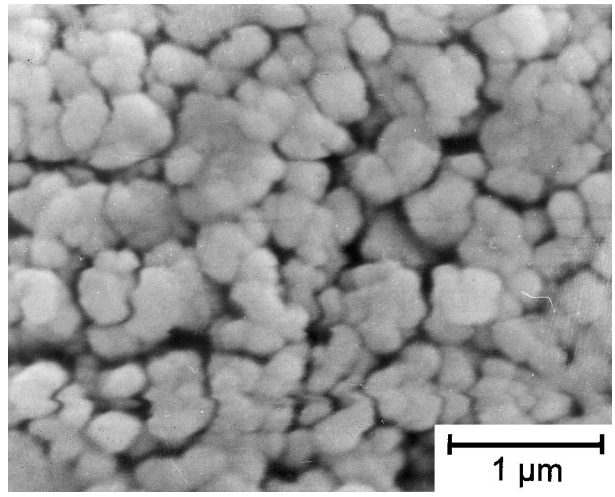

Fig. 2. SEM-image of UF-SiC powder with a mean particle-size of 0·51 μm.

Table 2. Density values obtained after compaction, hardening and cracking for each SiC powder

SiC-quality/ mean particle-size [μm]	*Density after compaction [g cm^{-3}]*	*Density after hardening [g cm^{3}]*	*Density after cracking [g cm^{-3}]*	*Theoretical density [g cm^{3}]*
F 500/12·8	1·95 (66·1%)	1·89 (64·2%)	1·85 (62·7%)	2·95 (100%)
F 800/6·5	1·89 (64·6%)	1·83 (62·5%)	1·79 (61·2%)	2·92 (100%)
F 1000/4·5	1·84 (63·0%)	1·78 (61·1%)	1·74 (59·8%)	2·91 (100%)
F 1200/3·0	1·80 (61·9%)	1·74 (60·0%)	1·71 (58·8%)	2·90 (100%)
UF 05/1·5	1·97 (66·3%)	1·92 (64·7%)	1.89 (63·8%)	2·97 (100%)
UF-10/0·9	1·86 (63·5%)	1·81 (61·7%)	1·79 (61·1%)	2·93 (100%)
UF-15/0·51	1·78 (61·1%)	1·72 (59·3%)	1.73 (59·6%)	2·91 (100%)
UF-45/0·24	1·62 (57·0%)	1·56 (54·9%)	1·58 (55·6%)	2·85 (100%)

grows on the original α-SiC particles. The pores of the green-compact are filled up with liquid silicon so that after infiltration a practically dense product ($>99\%$ of theoretical density) is obtained.

The infiltrated compact was then ground and cut with a diamond saw into bars measuring $40\times 3\times 4\,mm^3$. The bars were polished with diamond grit of a range of sizes down to $1\,\mu m$. The density of the infiltrated specimens was determined by Archimedes principle in water.

The fracture toughness of the composites was measured using three-point loading and single-edge notched beam technique with a notch width of $100\,\mu m$, a span of 11 mm and a cross head speed of $0{\cdot}5\,mm\,min^{-1}$ (9 specimens for every material). The broken bars of the fracture toughness measurement were used to determine bending strength. Bending strength was measured on $20\times 3\times 4\,mm^3$ bars (18 bars for every material) at room temperature using three point loading with a span of 11 mm and a cross-head speed of $0{\cdot}2\,mm\,min^{-1}$ and were evaluated using Weibull statistics. The number of tested bars is sufficient for determining the bending strength.

3 Results and Discussion

3.1 Density of the green-compact

Table 2 shows the measured densities of the green-compacts. Figure 3 represents the dependence of the green-compact-densities (% of theoretical density) after compaction, hardening and cracking on the particle-size of the used SiC. The theoretical densities were calculated based on the densities after cracking, the used volume fraction of α-SiC, the volume fraction of β-SiC formed of the stoichiometric reaction of carbon with silicon and the volume fraction of pores which are filled up with silicon during the infiltration process.[9]

In general, the use of UF-SiC resulted in higher pressed densities compared to the densities of the Fine-SiC-composites. This behavior is caused by the spherical shape of the UF-SiC-particles which leads to a better compaction during pressing.

However, with decreasing the SiC particle-size a clear decrease of the densities was seen. This circumstance can be explained by the higher specific surface of fine particles which leads to larger particle-friction during the compaction procedure and

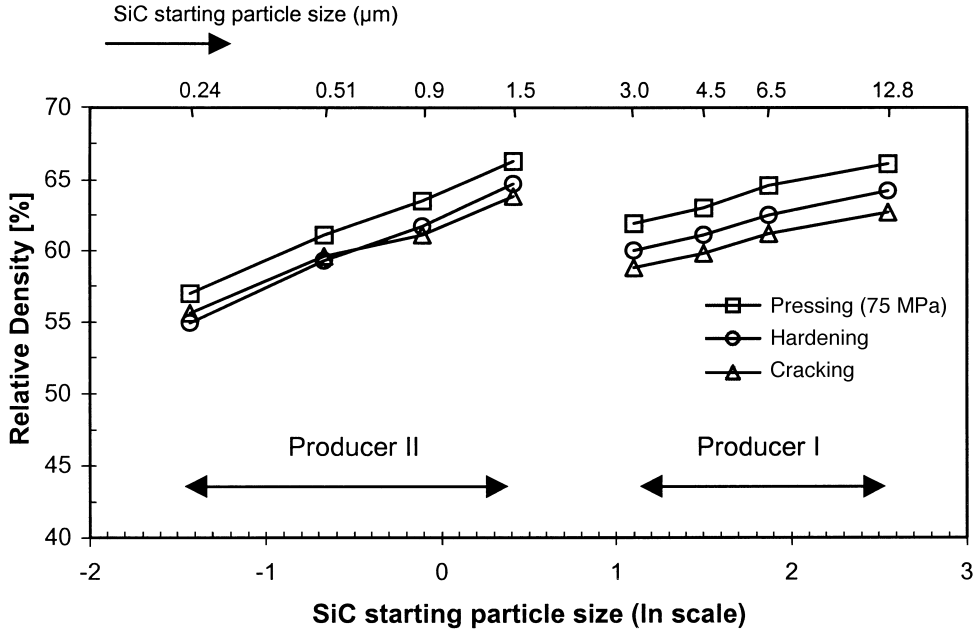

Fig. 3. Relative densities as a function of particle-size of SiC-powder in SiC–Si.

Table 3. Densities and free silicon content of the silicon infiltrated composites

SiC-quality/ particle-size [μm]	*Free silicon content (vol%)*	*Infiltrated density [g cm^{-3}]*	*Percentage of theoretical density [% o. Th.]*
F 500/12·8	30	2·94	99·8
F 800/6·5	32	2·92	100·0
F 1000/4·5	34	2·91	100·0
F 1200/3·0	36	2·89	99·7
UF 05/1·5	29	2·97	99·9
UF-10/0·9	31	2·93	100·0
UF-15/0·51	36	2·89	99·3
UF-45/0·24	55	2·56	89·5

subsequently to a loss of density. The observed decrease of the densities is more significant when using UF-SiC powder. This explains that the UF SiC-powders (especially powders with a particle-size of 0·51 and 0·24 μm) have a greater resistance to compaction than the Fine-SiC powders. The high content of SiC-agglomerates may also influence the behavior of these powders during compaction.

Figure 3 reveals that the cracking densities of the samples made of 0.51 and 0.24 μm UF SiC are higher than the densities observed after hardening. This is a consequence of the higher shrinkage after the cracking procedure.

3.2 Densities after infiltration

Table 3 shows the density-values observed after infiltration compared to the theoretical density. Almost fully dense composites were obtained using the Fine-SiC powders and the UF-SiC powders with a mean particle-size of 1·5 and 0·9 μm, respectively. The amount of pores is lower than 0·3%.

An infiltrated density of 99·3% of the theoretical density was received using the UF-SiC powder with

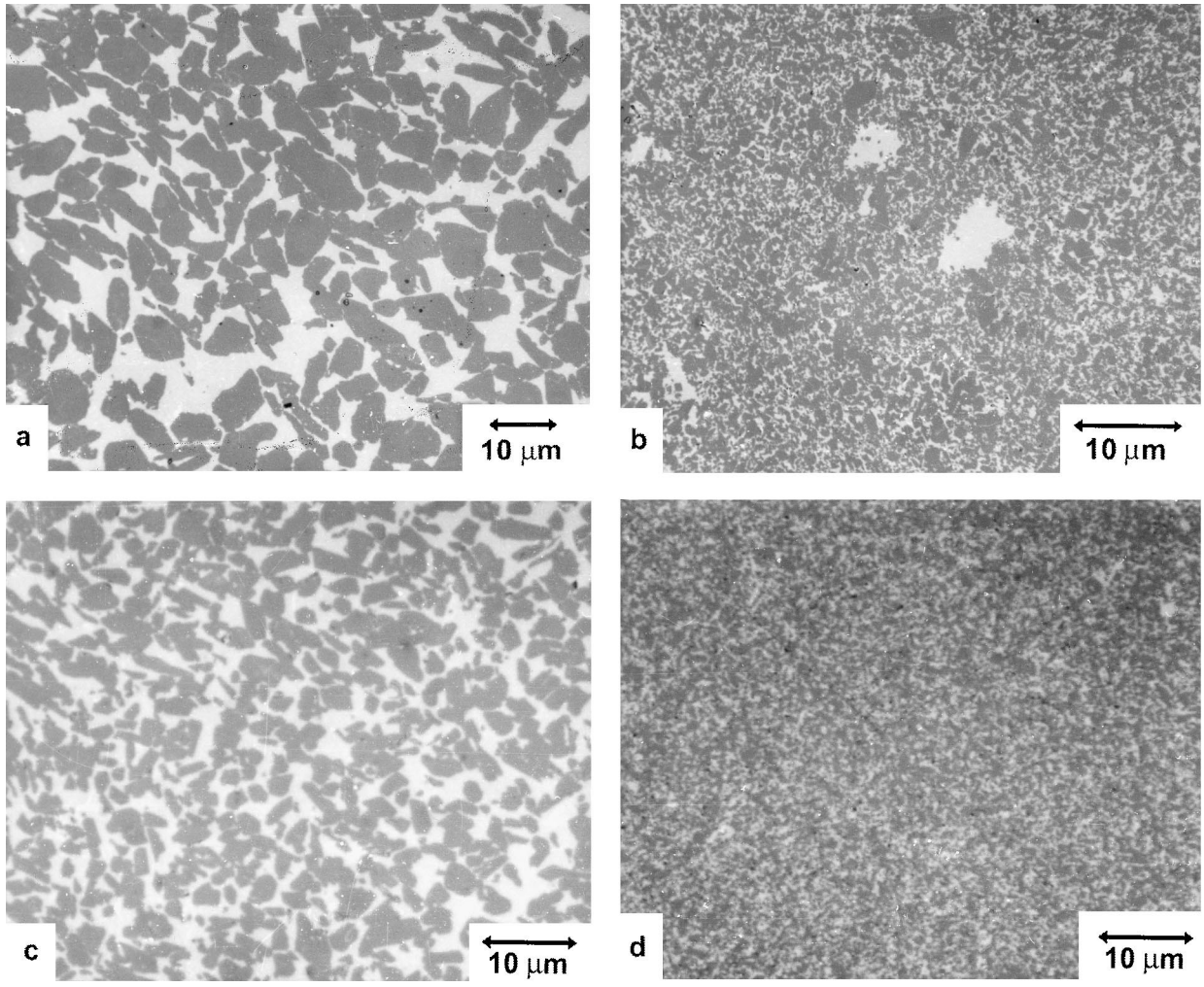

Fig. 4. Optical micrographs of SiC–Si illustrating homogeneous structure using (a) 12·8 μm Fine-SiC, (b) 1·5 μm UF-SiC, (c) 3 μm Fine-SiC and (d) 0·51 μm UF-SiC.

a mean particle-size of 0·51 μm. Compared to other SiC powders a high porosity of 10·5% was found using the 0·24 μm UF-SiC. It is assumed that the relatively high oxygen content of this SiC powder (4·5 wt%) causes the incomplete infiltration. During infiltration the SiO_2 layer on the SiC particles reacts with the free carbon as well as the liquid silicon. In both cases, gaseous products are produced (CO and SiO, respectively). These gases have a certain gas pressure and as a result hinder the liquid silicon to flow into the green-compact. The influence of the oxygen content on the infiltrated density can also be seen on the sample made of 0·51 μm UF-SiC. A porosity of 0·7 vol% is observed. Due to the very low oxygen content (<1 wt%) of the other SiC qualities no decrease of the densities was seen.

3.3 Microstructural analysis

Figures 4 and 5 show the microstructure of different SiC–Si samples. On Fig. 4 the light regions correspond to Si, and the gray regions to SiC. All illustrated micrographs show homogeneous structures of the composites unlike found by others.[12] As shown in Fig. 4(a) and (c), composites made of Fine-SiC powder are composed primarily of a continuous Si matrix with homogeneously dispersed grains of SiC. In contrast, composites made of UF-SiC consists of continuous SiC matrix with homogeneously dispersed Si, as shown in Fig. 4(b) and (d). All the samples are found to be fully dense. Figure 5 illustrates inhomogeneous areas of UF-SiC composites.

Due to an inhomogeneous compaction big silicon islands and cracks filled with silicon beneath homogeneous regions can be found in the microstructure of some UF-SiC powder composites. The inhomogeneous compaction resulted from the higher particle-size-friction of the UF-SiC during compaction and the lower plasticity of the produced granulate. These inhomogeneous areas were found in both, the Fine-SiC and UF-SiC composites, but the frequency is much higher in UF-SiC than in Fine-SiC composites [Fig. 5(a) and (b)].

Microstructural analysis of composites produced from UF-SiC powder reveals extraordinary big and well crystallised SiC particles [Fig. 5(c) and (d)]. In general, these giant SiC particles are observed

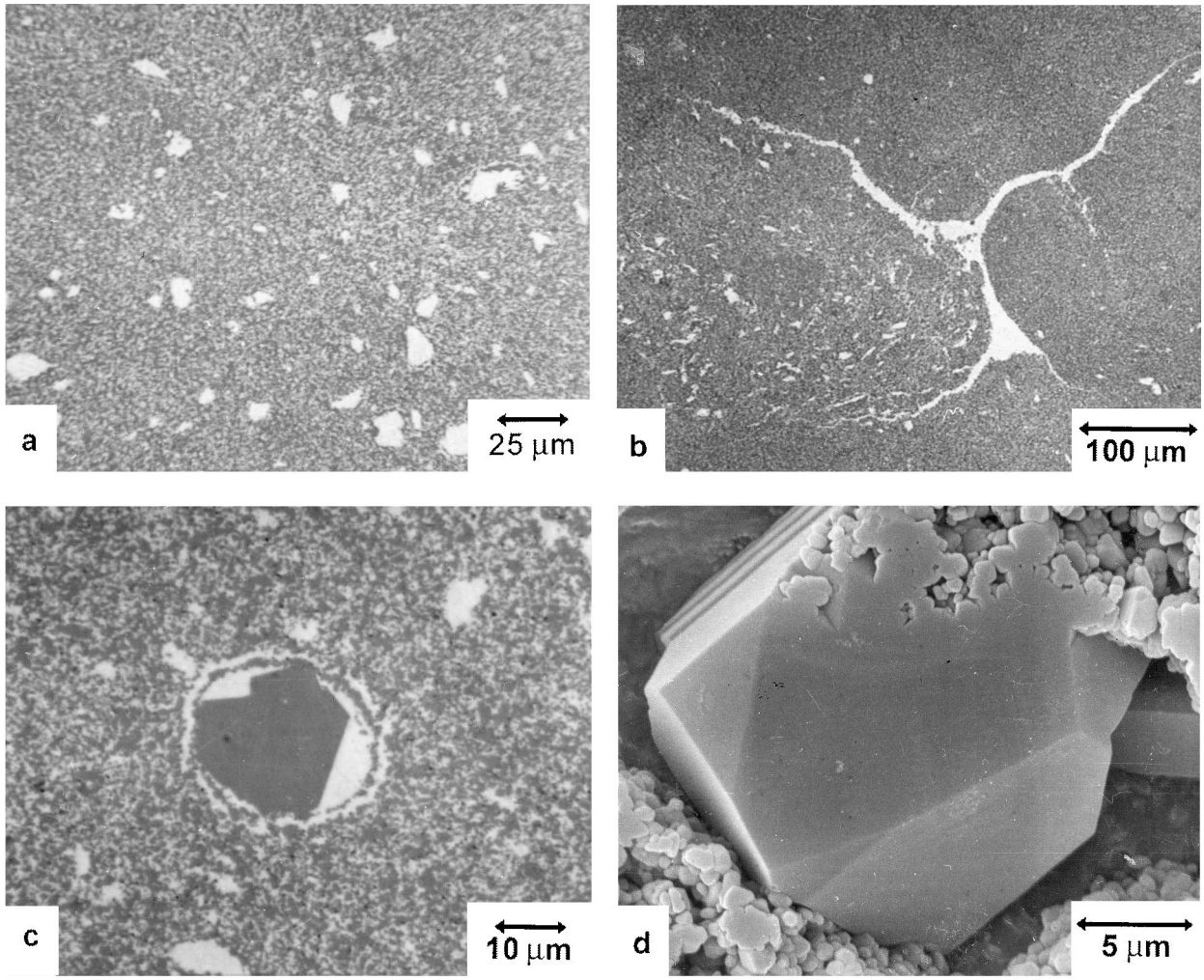

Fig. 5. Micrographs of SiC–Si illustrating failures in the structure. (a) silicon islands, (b) cracks filled with silicon, (c) and (d) giant particle growth [in (d) silicon is removed with sodium hydroxide].

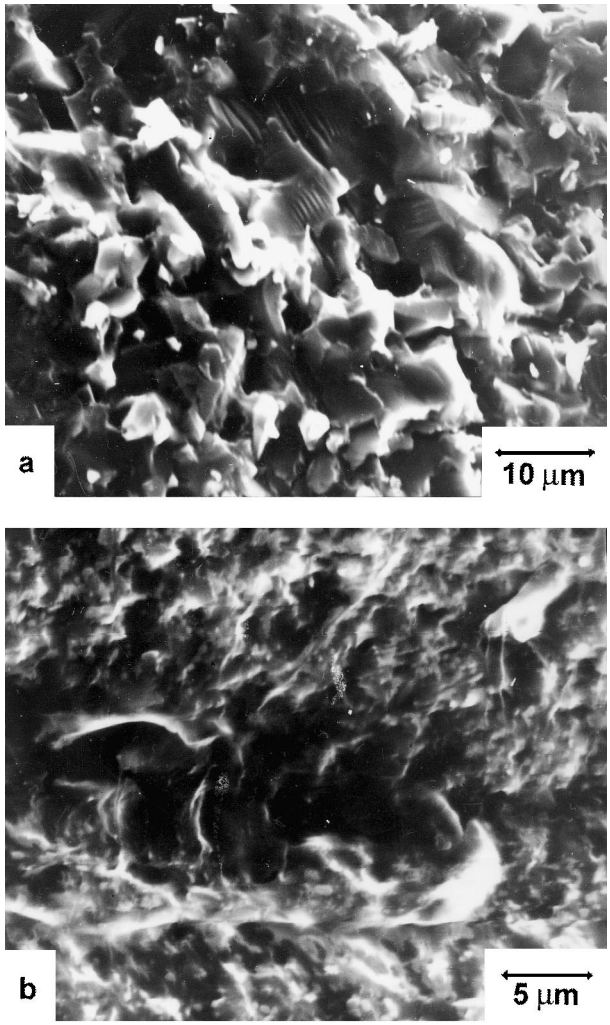

Fig. 6. SEM-micrographs of the fracture surface of SiC–Si made of Fine-SiC ((a), 6·5 μm) and UF-SiC ((b), 1·5 μm).

only in UF-SiC composites and as SEM investigations showed were not found in the supplied SiC powders. It is supposed that these giant SiC particles are built as a consequence of solving and dissolving processes during the infiltration. Small SiC particles are solved in liquid silicon and subsequently, when the silicon is saturated with SiC, are dissolved again on a bigger SiC particle. Around such SiC particles a SiC-free silicon area can often be found. However, during the infiltration process no grain growth of the starting SiC powder occurs.

All fracture surfaces are observed in a SEM to determine the mode of fracture in the composites. It can be seen that the fracture is combined trans- and intergranular failure. In Fig. 6(a) some striation marks are seen along the cleavage plane of the silicon. These striation marks are similar to those found in the system WC-Co[13] and are probably the result of a pile-up of dislocations during failure. In Fig. 6(b) a crack within the microstructure is shown. However, the crack planes are partially held together by silicon phase indicative of extensive crack bridging.

3.4 Mechanical properties

The mechanical properties of the composites are shown in Table 4. The dependence of the fracture toughness and mean bending strength as a function of the particle-size of α-SiC are demonstrated in Figs 8 and 9, respectively.

Due to its low density after infiltration no testing of the mechanical properties of the composite made of 0·24 μm SiC powder were carried out.

In the case of UF-materials provided by producer II (mean SiC particle size $< 1.5\,\mu$m) the toughness values of the composites show an increase with increasing starting particle size. In materials toughened by crack bridging such an increase is expected due to the increasing length of the bridges with a coarsening of the microstructure. For these materials the bending strength also increases with increasing size of SiC starting particles, the ratio of K_{Ic}/σ_B remains more or less constant. This indicates for all three composites investigated an almost equal size of the fracture initiating defects which can be calculated using the Griffith failure criterion

$$\sigma * Y * \sqrt{\pi * a} \equiv K \geq K_{Ic}$$

where σ is the load amplitude, a the crack length, Y a geometric factor, K the stress intensity factor and K_{Ic} the fracture toughness. Using this equation the critical defect radius is

$$a_c = \frac{1}{\pi} * \left(\frac{K_{Ic}}{Y\sigma_B}\right)^2$$

Table 4. Mechanical properties of the SiC–Si composites

SiC-quality/ particle-size [μm]	*Fracture toughness [$MPa\sqrt{m}$]*	*Mean Bending strength σ_{B50} [MPa]*	*Critical defect size a_c [μm]*	*Weibull modulus m*
F 500/12·8	3·7 ± 0·2	415	66	11
F 800/6·5	3·6 ± 0·2	479	49	11
F 1000/4·5	4·1 ± 0·4	521	42	15
F 1200/3·0	3·8 ± 0·5	548	38	11
UF 05/1·5	4·3 ± 0·4	583	42	8
UF-10/0·9	3·7 ± 0·4	535	38	8
UF-15/0·51	3·1 ± 0·7	453	37	7

with σ_B as the fracture strength and $Y = 2/\pi$ for a penny shaped short crack. The critical defect diameter is about 40 μm for all three materials. The investigation of the fracture surfaces revealed that all fractures originated from defects near the surfaces (circled area in Fig. 7, left) and the defect-diameters are in the range of 50–70 μm. It is interesting to note that the size of the defects does not depend on the size of the SiC starting powders. EDS investigations have shown that the defect in Fig. 7 is a big silicon-island (bright area in Fig. 7 right) with small amounts of β-SiC. Under this silicon island a large pore and inside the pore needles were found. These needles may either be silicon- or silicon carbide whiskers. It is assumed that as a consequence of a special environment within the pore (vacuum and temperature) the whiskers had grown by a CVD process during the infiltration process.

It can be assumed that the defects found are a consequence of an imperfect processing technology. It may be possible that during the mixing step, with the tumbling mixer, a homogeneous distribution of the soot cannot be achieved and as a consequence carbon islands remain after compaction. The fast reaction of carbon with liquid silicon forms β-SiC. The β-SiC grows into the pores (which are necessary for a successful infiltration) of the compacts and hence lowers the porosity of the composites. However, it is assumed that due to a fast growth of β-SiC some pores are not fully closed and as a result big pores which are partially filled with silicon are obtained.

In the case of the composites made of SiC powder provided by producer I the toughness is independent on the SiC starting particle size and remains constant at 3·8 MPa$\sqrt{\text{m}}$. The bending strength clearly increases with decreasing SiC particle size. The critical defect radius increased with increasing SiC particle size, a mathematical analysis gives that $a_c = kd^{0,4}$ (d is the diameter of the starting SiC particles) and the strength is $\sigma_B = kd^{-0.2}$ with k a material constant. Fractographic observations showed that the failures originated at edges and surface flaws which are possibly made during machining. The size of these flaws increases with increasing SiC starting particle size.

Summarised it can be said that in this investigation the maximum strength value (583 MPa) was found using the UF-powder with a mean particle-size of 1·5 μm. This strength value is 2 times higher than the strength values found in[7] at comparable silicon contents and about 3 times higher than a commercial product. In general all the bending strength values obtained are higher than the strength values reached in previous works with composites made of two SiC powders with two different grain sizes (so called bimodal grain structure).

It may be assumed that the following effects influence the mechanical properties of the composites and should be taken into consideration:

- differences in the shape, particle-size distribution and agglomeration of the starting SiC powders;
- oxygen content of the starting SiC powders;
- density of pressing defects;
- abnormal particle-growth caused by secondary crystallisation;
- internal stresses.

The enhanced agglomeration of the UF-SiC influences the SiC–Si composites most during the production of the SiC-C granulate and the subsequent compaction procedure. It is inferred that in the case of using UF-SiC the mixing in a tumbling

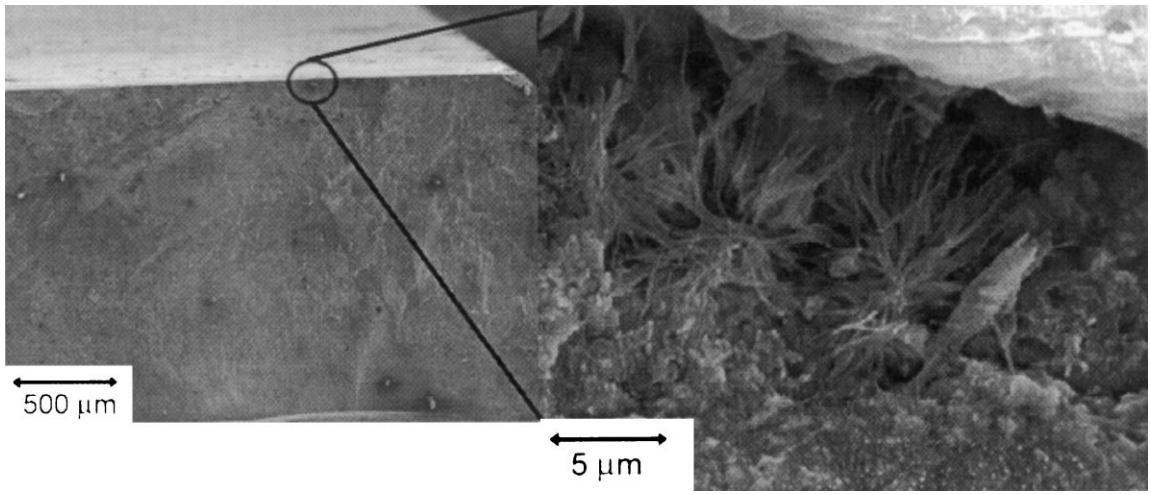

Fig. 7. SEM-micrographs of the fracture surface of SiC–Si made of UF-SiC (1·5 μm). Circled area indicates origin of fracture (left). Detail of the origin of fracture with whiskers (right).

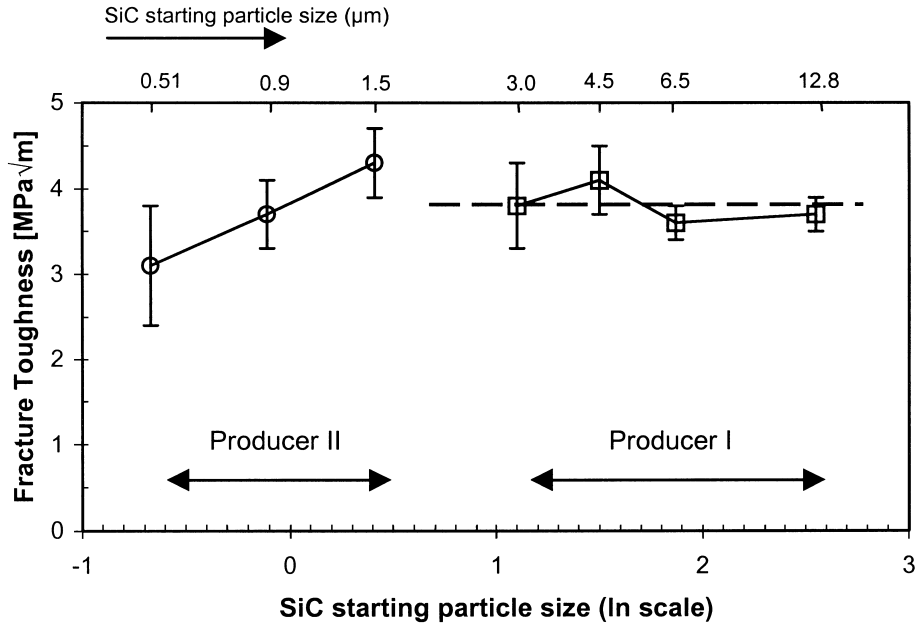

Fig. 8. Fracture toughness versus particle-size of α- SiC-Powder in SiC–Si.

mixer is not sufficient. A change to another mixing method (e.g. attritor milling) should be taken into consideration. The provided SiC powders (producer I and II) show clear differences in their manufacturing history, in the particle-morphology, particle-size-distribution, the oxygen content and differences in the extend of SiC-agglomeration. It is assumed that because of these differences the mechanical properties obtained of the composites made of Fine-SiC and UF-SiC, respectively, cannot be directly compared.

The influence of oxygen content is seen in the decrease of the densities of the samples produced of Ultra-Fine SiC-powder with a particle-size-size of $0{\cdot}5\,\mu$m. In further investigations the oxygen content of the used SiC powders should be decreased by etching with hydrofluoric acid or sodium hydroxide. However, a low content of oxygen (a thin layer of SiO_2) is necessary for a complete infiltration.[14] During infiltration the molten silicon reacts with the silica under formation of SiO. The SiO itself reacts with the surface-near carbon and opens in that way surface-near pores.

The increased density of pressing defects and the size of defects are the main influence on mechanical properties. Because of the smaller grain size of the UF-SiC powders the pressing-failure-density is

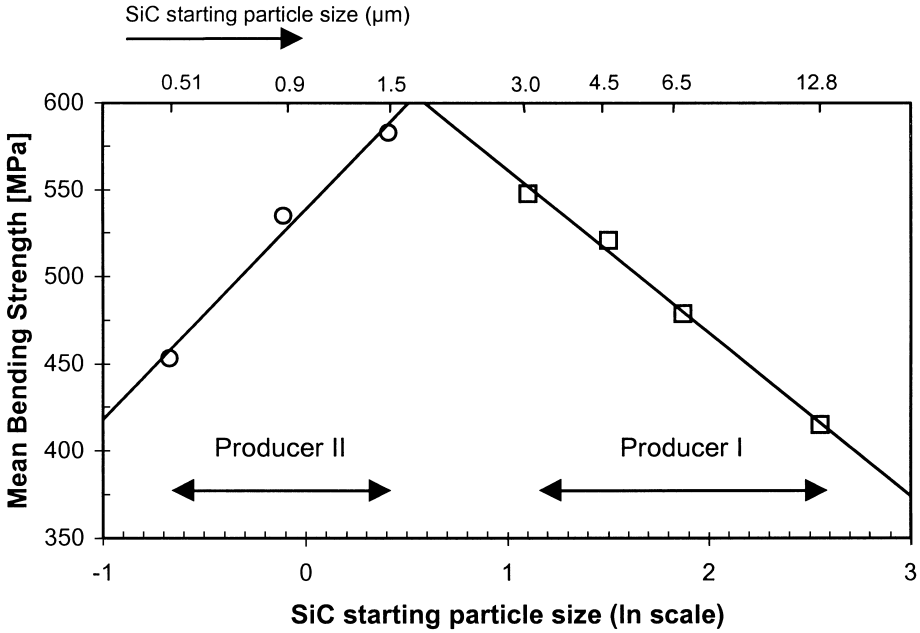

Fig. 9. Mean bending strength versus particle-size of α-SiC-Powder in SiC–Si.

typically higher than using Fine-SiC powders. Despite this fact, the composite made of UF-SiC powder (1·5 μm) shows higher values of strength and toughness than the sample made of Fine-SiC powder (F1200, 3 μm). However, all defects found in the UF-microstructures are situated near the surfaces and have a size in the range of 50–70 μm.

The giant particles found have no influence on the mechanical properties. Due to the small size, these particles do not act as origins of cracks. However, the growth of the giant particles can be influenced on the one hand by controlling the temperature during infiltration process and on the other hand by reducing the temperature of homogenisation during infiltration. This leads to a decrease in the solubility of SiC in silicon and therefore the tendency of anisotropic particle-size-growth.

The stress inside the UF-microstructures is caused by the expansion of silicon during cooling down and has been described in earlier works.[15,16]

4 Conclusions

In this investigation 8 α-SiC powders supplied by two producers were used. Producer I provided SiC powders with mean particle-sizes in the range of 12·8–3 μm, the mean particle sizes of SiC powders provided by producer II were in the range of 1·5–0·24 μm.

To summarise, it can be said that no increase of the mechanical properties was achieved using SiC powders provided by producer II. The critical defect size is about 40 μm for all these materials and does not depend on the size of the SiC starting powders. The investigation of the fracture surfaces revealed that all fractures originated from defects near the surfaces.

The use of SiC powders provided by producer I showed that the bending strength and the critical defect radius, respectively, increased with decreasing SiC particle size. In this investigation the maximum mean bending strength of 583 MPa was reached using UF-SiC with a mean grain size of 1·5 μm. It has to be noted that the fracture toughness of all investigated samples remains constant at 3·8 MPa$\sqrt{\text{m}}$.

Acknowledgements

The authors would like to thank Professor Dr. R. Danzer and Dipl.-Ing. T. Lube (both University of Leoben) for their help and discussions. We greatly acknowledge the support of this work by the Jubiläumsfonds der Österreichischen Nationalbank, Project No. P4877 and P6281.

References

1. Luthra, K., Singh, R. and Brun, M., Toughened silcomp composites—process and preliminary properties. *Am. Ceram. Soc. Bull.*, 1993, **72**(7), 79–85.
2. Wei, G. and Tennery, V., Evaluation of tubular ceramic heat exchanger materials in residual oil combustion environment, ORNL/TM-757, March, 1981.
3. Trantina, G., Design techniques for ceramics in fusion reactors. *Nucl. Eng. Des.*, 1979, **54**(1), 676–677.
4. Forrest, C., Kennedy, P. and Shennan, J., The fabrication and properties of self-bonded silicon carbide. *Special Ceramics*, 1972, **5**, 99–123.
5. Lim, C. and Iseki, T., Transport of fine-grained β-SiC in SiC/Liquid Si system. *Adv. Ceram. Mater.*, 1988, **3**, 291–293.
6. Krauth, A. *et al.*, Ingenieurkeramische Bauteile für Anwendungen in der Energietechnik, Verfahrenstechnik, Metallurgie und Motorenbau. *Keramische Komponenten für Fahrzeug-Gasturbinen* Vol. III, Springer Verlag, 1984, pp. 647.
7. Chakrabati, O., Ghosh, S. and Mukerji, J., Influence of grain size, free silicon content and temperature on the strength and toughness of reaction-bonded silicon carbide. *Ceramics International*, 1994, **20**, 283–286.
8. Schmid, W., Brohs, F., Hörhager, S. and Wruss, W., Einfluß der Dichte und Korrtgröße auf die Biegefestigkeit von siliziuminfiltrierten Siliziumcarbid. *Werkstoffe und Konstruktion*, 1991, **5**(2), 118–123.
9. Schmid, W., Beitrag zur Entwicklung modifizierter SiSiC-Me Cermets, Dissertation, TU-Wien (1988).
10. Blecha, M., Schmid, W., Krauth, A. and Wruss, W., Herstellung grobkörniger, auf hohen SiC-Gehalt otimierter, SiC-C-Grünkörper für die Herstellung von SiSiC. *Sprechsaal*, 1990, **123**(3), 263–268.
11. Chang-Bin, L. and Takayoshi, I., Formation and transportation of intergranular and nodular fine grained β-SiC in reaction sintered SiC. *Adv. Ceram. Mater.*, 1983, **3**(6), 590.
12. Zhou, H., Webb, J. and Singh, R., Elevated temperature mechanical properties of compositionally varied Si/SiC composites. *Ceram. Trans.*, 74, (Advances in Ceramic-Matrix Composites III), 411–422.
13. Sigl, L., Mataga, P., Dalgleish, B., McMeeking, R. and Evans, A., On the toughness of brittle materials reinforced with a ductile phase. *Acta metall.*, 1988, **36**(4), 945–953.
14. Forrest, C. W., Kennedy, P. and Shennan, J. V., The fabrication and properties of self-bonded silicon carbide bodies, TRG Report 2053 (S), 1970.
15. Gmelins Handbuch der anorganischen Chemie, Teil 15 B (Silizium), Verlag Chemie, Auflage, 63–65 Berlin, 1959.
16. Cohrt, H., Herstellung, Eigenschaften und Anwendung von reaktionsgebundeni siliziuminfiltriertem Siliziumcarbid, Werkstofftechnik, 1985, 16, 277–285.